Shape of Clusters of Galaxies as a Probe of Screening Mechanisms in Modified Gravity

Claudio Llinares and David F. Mota
Institute of Theoretical Astrophysics, University of Oslo, N-0315 Oslo, Norway
(Received 29 May 2012; published 9 April 2013)

Scalar fields are crucial components in high energy physics and extensions of general relativity. The fact that they are not observed in the Solar System may be due to a mechanism which screens their presence in high dense regions. We show how observations of the ellipticity of galaxy clusters can discriminate between models with and without scalar fields and even between different screening mechanisms. Using current x-ray observations we put novel constraints on the different models.

DOI: 10.1103/PhysRevLett.110.151104 PACS numbers: 04.50.Kd, 04.80.Cc, 98.65.Cw

General relativity (GR) is a successfully tested theory at solar system scales and below. Assuming that this theory is valid also at cosmological scales gave rise to the ΛCDM model, which has its foundations in two unknown components: dark matter and dark energy. The nature of these two components could therefore be an indication of the breakdown of Einstein's gravity on large scales. This has motivated the proposal of several theories which modify GR at astrophysical scales [1].

An imperative requirement to all modified gravity proposals is that they all must recover GR in the Solar System. This is done via a screening mechanism. Presently, there are three main screening mechanisms: Vainshtein [2], symmetron [3], and chameleon [4]. We focus on the two later ones since they are described by scalar degrees of freedom, and they have the common feature of emerging at the onset of nonlinear structure formation.

The key feature of a screening mechanism is to switch off the extra degrees of freedom inside matter overdensities (small scales), and to switch them on in the cosmological background (large scales). When the scalar fields are *on* a fifth force emerges between the matter particles. When it is *off* (the field is screened) the fifth force disappears and GR is recovered. This is a highly nonlinear process, since the scalar fields are strongly coupled to matter and have highly nonlinear bare potentials.

The aim of this Letter is to investigate signatures that the chameleon and the symmetron fields imprint in the formed nonlinear structures, which can be measured by current experiments, and so be used as probes of extensions of GR and the required screening mechanism to reproduce it within the Solar System.

Dark matter halos are not spherical, and their density scales differently along the x, y, or z directions. Such an anisotropic shape of the halos (ellipticity), leads to an anisotropic screening mechanism of the scalar fields. The result is that the fifth force between dark matter particles can be present in one direction, while being almost nonexistent in another. This anisotropy may lead to an increase in the ellipticity of the clusters, which can be measured by lensing or x-ray observations, and so be used as tracers of the inherent screening mechanism.

It is well known that the Newtonian potential of triaxial systems acquires a shape that is more spherical than the matter-density distribution itself (see for instance results from simulations in Lau *et al.* [5]). In the case of strongly coupled scalar fields their isosurfaces are expected to follow closely the matter-isodensity contours. Due to the screening, the fifth force range and couplings change along the matter-isodensity contours, leading to modifications in the shape of the system. In this Letter we test this conjecture by studying the 3D distribution of scalar fields that correspond to triaxial dark matter halos, and use x-ray observations to put bounds on the models with and without scalar fields and to distinguish between different screening mechanisms.

We present calculations of the scalar fields and Newtonian potential for a fixed density distribution. Therefore, our study will not account for the time evolution of the system, which can be seen as a restriction in our results. Nevertheless, one has to take into account that the x-ray component of relaxed clusters is in hydrostatic equilibrium and thus, their shape follows that of the total gravitational potential (GR + modifications). By making our calculations for two different shapes of the underlying dark matter (DM) distribution, we show that whatever is the effect of modified gravity in the system while virialized, the relative difference with respect to GR is not very sensitive to the shape of the underlying DM distribution. Therefore, the result is not expected to be sensitive to the time evolution. This must be confirmed with cosmological simulations, which go beyond this work.

The Newtonian potential ϕ_N is given by

$$\nabla^2\phi_N = \frac{3}{2}\frac{\Omega_m H_0^2}{a}\delta, \tag{1}$$

where δ is the overdensity defined as $\delta\rho/\rho_b$, ρ_b is the mean density of the Universe, ϕ_N is the perturbation in the metric, Ω_m is the mean density of the Universe in terms of the critical density, H_0 is the Hubble constant, and a is the expansion factor.

The symmetron model is defined by the following effective potential:

$$V_{s,\mathrm{eff}}(\phi_s) = \frac{1}{2}\left(\frac{\rho}{M^2} - \mu^2\right)\phi_s^2 + \frac{1}{4}\lambda\phi_s^4, \quad (2)$$

which leads to the following equation of motion in the static limit:

$$\nabla^2\phi_s = a^2\left[-\mu^2\phi_s + \lambda\phi_s^3 + \frac{1}{M^2}\rho\phi_s\right], \quad (3)$$

where μ and M are mass scales, ρ is the matter density and λ is a length scale. We normalize the field ϕ_s with the minimum of the potential $\phi_{s,0}$ that corresponds to zero density and is given by: $\phi_{s,0}^2 = \frac{\mu^2}{\lambda}$. By dividing the whole equation by $\phi_{s,0}$, defining the dimensionless quantity $\chi_s = \frac{\phi_s}{\phi_{s,0}}$, and taking into account that $\rho_{\mathrm{SSB}} = M^2\mu^2$ at z_{SSB}, we get

$$\nabla^2\chi_s = \frac{a^2}{2\lambda_{s,0}^2}\left[-\chi_s + \frac{\eta\chi_s}{a^3(1+z_{\mathrm{SSB}})^3} + \chi_s^3\right], \quad (4)$$

where η is the matter density field normalized with the mean density of the Universe, and $\lambda_{s,0} = \frac{1}{\sqrt{2}\mu}$ is the range for the field that corresponds to zero density.

The associated effective potential for the chameleon model is

$$V_{c,\mathrm{eff}}(\phi_c) = M_c^{4+n}\phi_c^{-n} + \rho e^{\beta\phi_c/M_{\mathrm{pl}}}, \quad (5)$$

where M_c has units of mass, β is dimensionless, n is a positive constant and M_{pl} is the Planck mass. The linearized equation of motion for the scalar field is

$$\nabla^2\phi_c = -\frac{nM_c^{4+n}}{\phi_c^{n+1}} + \frac{\beta}{M_{\mathrm{pl}}}\rho. \quad (6)$$

As in the symmetron model and for numerical convenience, we normalize ϕ_c with the minimum of the effective potential $\phi_{c,0}$. In the chameleon case, the minimum diverges when the density goes to zero. Thus, in this case we normalize with the minimum that corresponds to the mean density of the Universe. After including the range of the field for this particular density

$$\lambda_c^2 = \left(\frac{dV_{c,\mathrm{eff}}}{d\phi_c}\right)^{-1} = [n(n+1)M_c^{4+n}\phi_{c,0}^{-(n+2)}]^{-1} \quad (7)$$

and renormalizing the field $\chi_c = \phi_c/\phi_{c,0}$, we get

$$\nabla\cdot[q\omega_c^{q-1}\nabla\omega_c] = \frac{1}{(n+1)\lambda_c^2}\left[\eta - \frac{1}{\omega_c^{q(n+1)}}\right], \quad (8)$$

where $\chi_c = \omega_c^q$ is chosen to facilitate the numerics.

To solve the field equations we use a Fourier based method for the Newtonian case and an implicit multigrid nonlinear solver for both scalar field equations. The code uses a uniform grid and is an extension of Ref. [6], to which we added both scalar field solvers. The boundary conditions are periodic. The three solvers were tested successfully against analytic solutions for a sphere of uniform density located in the center of the box.

To test the possibility that the presence of a scalar field can have an impact in the shape of clusters, we calculated the Newtonian potential and both scalar fields for a density distribution given by a NFW profile [7]. The virial radius R_v of the object was fixed to 1 Mpc/h, which corresponds to an object of 10^{14} $M_\odot$ (i.e., a cluster of galaxies). Following mass-concentration relations coming from simulations [8], we choose a concentration of 6.3 for our halo. The density distribution was defined in every node of the grid following the analytic profile. The size of the box is 16 Mpc/h and 512 nodes per dimension were employed, which corresponds to a spatial resolution of about 30 kpc/h. The underlying cosmology needed to normalize the density profile was chosen as ΛCDM, defined by $\Omega_m = 0.3$ and $H_0 = 70$ km/ sec/Mpc. All our analyses are at redshift $z = 0$.

As we want to measure how closely the scalar field follows the triaxiality of the density distribution, we need to assume a density profile. We choose the NFW profile

$$\frac{\rho(r)}{\rho_0} = \frac{\delta_{\mathrm{char}}}{\Omega_0}\frac{1}{(r/r_s)(1+r/r_s)^2}, \quad (9)$$

but using an ellipsoidal radius $k = \sqrt{x^2 + \frac{y^2}{q^2} + \frac{z^2}{s^2}}$ instead of the radius r that corresponds to spherical coordinates. The axial ratios of the density distribution where fixed to be $(q^2, s^2) = (0.5, 0.3)$.

Our calculations show that the chameleon model is sensitive to the behavior of the density far from the center of the halo. In order to get stable results, we immersed the halo in a background with a constant density of 0.4 times the mean density of the Universe. We choose a value lower than the mean density of the Universe to take into account the fact that clusters are surrounded by voids, and thus immersed in underdense regions. In fact, we find that the Newtonian and symmetron values are independent of the presence of this background.

Given the solutions of the field equations, we now measure the shape of their isosurfaces: the axial ratios of the isosurfaces of a given distribution f (in our case the Newtonian potential and both scalar fields) are

$$M_{ij} = \int f x_i x_j d^3x. \quad (10)$$

As the absolute value of the scalar fields does not decrease with radius, we defined f as a renormalized version of the fields. These isosurfaces can be approximated by ellipsoids, described by the ellipsoidal radius k with axial ratios $q^2 = \frac{M_{xx}}{M_{zz}}$ and $s^2 = \frac{M_{yy}}{M_{zz}}$, where M_{xx}, M_{yy}, and M_{zz} are the eigenvalues of M_{ij}. The integral in that equation is computed by summing over the grid up to twice the virial radius. As in the symmetron model the scalar field can be

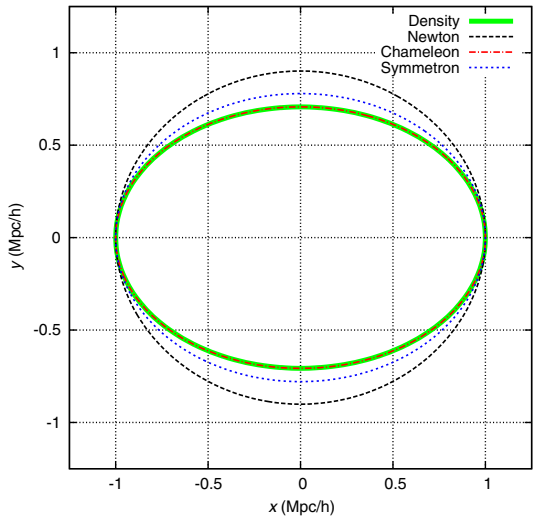

FIG. 1 (color online). Contours of density distribution, Newtonian potential, and symmetron and chameleon fields for the triaxial halo in the x-y plane. The contours where chosen such that all of them pass through the point (R_v, 0, 0). Here $z_{\rm SSB} = 1.6$ and $\lambda_{s,0} = \lambda_c = 1.1$.

screened inside regions given by values of k as large as $2R_v$, we extended the domain of the integral for the most extreme cases (with very small values of $\lambda_{s,0}$ and $z_{\rm SSB}$). Thus, in the symmetron case, we integrated up to the maximum between $2R_v$ and the radius k at which f reaches 0.5. In all the cases, the summation was made up to no more than $3R_v$. The shape of the region in which the integral is computed was obtained iteratively as in Ref. [9].

Figure 1 shows isodensities and isosurfaces for the Newtonian potential and both scalar fields in the plane that correspond to the major and intermediate axis of the system. As expected, the Newtonian isopotential falls apart from the matter-isodensities and acquires a form that is much closer to sphericity. In the scalar field cases, we find not only that their isosurfaces follow the density distribution much closer than the Newtonian potential, but also that there are differences between them (even when the range of the field is the same for both models).

We find that symmetron fields tend to be more spherical than the chameleons. The reason for such a difference lies in the mechanism driving the screening of the fifth force: in the symmetron there is a defined threshold density above which the field decouples from matter (the fifth force vanishes), while in the chameleon the fifth force disappears slowly and continuously (its range becomes shorter) as the density becomes higher and higher.

To quantify the differences between the models and understand the dependence of the result with the model parameters, we calculate the axial ratios for every model. The values obtained for the Newtonian potential are $q^2 = 0.84$ and $s^2 = 0.76$, which differ considerably from the input parameters given for the density. The results obtained for the symmetron and chameleon models are shown in Fig. 2. To make a fair comparison we show here the results as a function of the range of the field λ_s and λ_c that corresponds to the mean density of the Universe in both cases. We find a different behavior for each scalar field model. The symmetron mechanism tends to give more spherical isosurfaces when increasing both λ_s and $z_{\rm SSB}$. The chameleon mechanism is insensitive to changes in λ_c up to ranges that are larger than the virial radius itself. Once again, this reflects the difference in the way the fields are screened.

To test the stability of our calculations, we made resolution and box size convergence tests by increasing the resolution by a factor of two while keeping the box size constant and also by increasing both box size and resolution by the same factor. The tests were made for model parameters that are representative of isosurfaces with small and large values of q^2 and s^2. We find that our solutions are independent of the resolution. The Newtonian and

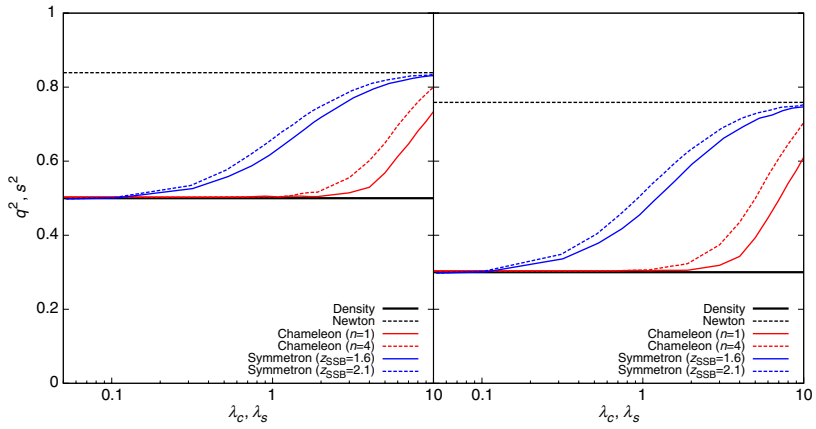

FIG. 2 (color online). Axial ratios q^2 (left) and s^2 (right) for the Newtonian potential and the two implementations of the scalar field as a function of the range of the scalar field. The two curves for the symmetron model correspond to two different values of $z_{\rm SSB}$. In the case of the chameleon model, we show results for two different values of n. The continuous black lines are the values that correspond to the density distribution and the dashed black lines the ones that correspond to the Newtonian potential.

symmetron solutions are stable with respect to changes in the box size. In the case of the chameleon model, we find that the solution is much more sensitive to the distance between the halo and the boundary. Nevertheless, the actual change in the axial ratios when going from 16 to 32 Mpc/h in the box size is only of the order of 5%, which is far from the variations we see when changing from model to model. In any case, the environment around nonisolated clusters is expected to change the solutions, but not the bulk of the signal.

To test the sensitivity of our results when the underlying density distribution is changed, we repeated our analysis with a less extreme model taken from simulations [10]: $(q^2, s^2) = (0.6241, 0.459\,684)$. We find that our results (the relative difference between the shape of the scalar field and that of the density) are rather insensitive to the underlying density distribution.

An estimation of the importance of the effect from the observational point of view can be made under the assumption that the x-ray component follows the isosurfaces of the total potential (Newtonian plus scalar field). The ellipticity $\epsilon = 1 - b/a$ of the projection on the sky of these isosurfaces should then be the same as of the gas density distribution. This assumption also makes it possible to obtain constraints on the model parameters, since there is a set of parameters for which the difference between the ellipticity that we predict by assuming standard gravity and by including the fifth force is larger than the errors in present x-ray observations. Lau *et al.* [11] reported measurements of ellipticities using Chandra and ROSAT observations originally presented in Vikhlinin *et al.* [12]. They found almost constant ellipticities in the radial range of $0.05 \lesssim r/r_{500} \lesssim 1$ which are given by $\epsilon \approx 0.18 \pm 0.05$. We refer the reader to Lau *et al.* [11] and references therein for details on these observations.

The calculation of the total potential was made by taking into account that the geodesics equation at redshift $z = 0$ has the following form in the symmetron case:

$$\ddot{\mathbf{x}} + 2H\dot{\mathbf{x}} + \nabla\left(\phi_N + 6H_0^2\Omega_m\lambda_{s,0}^2\frac{(1+z_{\rm SSB})^3}{2}\beta^2\chi_s^2\right) = 0,$$

and can be written for the chameleon as

$$\ddot{\mathbf{x}} + 2H\dot{\mathbf{x}} + \nabla\left(\phi_N + 6H_0^2\Omega_m\lambda_c^2\frac{(n+1)}{2}\beta^2\chi_c\right) = 0.$$

We estimate the ellipticity of these isosurfaces of total potential by taking the mean value over random projections. Figure 3 shows contours of the relative difference $\Delta\epsilon/\epsilon_N$ between ellipticities that correspond to the total potential associated to the modified models and to the Newtonian potential. The regions from black to light gray correspond to values larger than three, two, and one times $\sigma_{\rm obs}/\epsilon_{\rm obs}$. In other words, the black region is ruled out with more than $3\sigma_{\rm obs}/\epsilon_{\rm obs}$. When making this comparison, we assume that observations and Newtonian theory give the same values for the ellipticity. By taking into account a possible bias of the predictions of the standard model towards more spherical halos [11], one can relax slightly the constraints and include models with higher values of β that are excluded here.

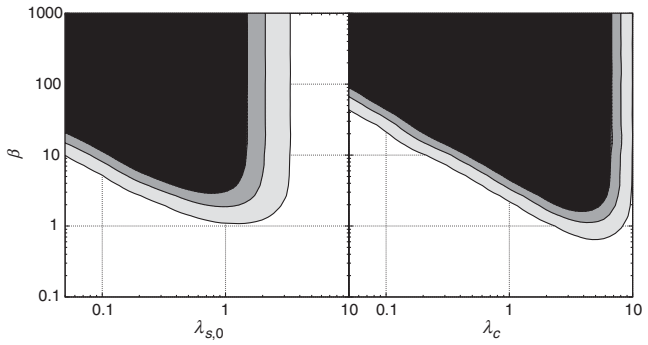

FIG. 3. Contours of relative difference $\Delta\epsilon/\epsilon_N$ between ellipticities that correspond to the modified models (Left: symmetron model, Right: chameleon model) with respect to Newtonian gravity. At small λ the screening mechanism emerges and the allowed parameter space increases. Here $z_{\rm SSB} = 2.1$ and $n = 4$.

From Fig. 3, it is clear that for high couplings and small ranges, the chameleon model is less constrained than the symmetron. In other words, the chameleon model tends to give more spherical objects. That seems to be in tension with Fig. 2: in there, the symmetron field tends to be more spherical. This can be understood taking into account the dependence on $z_{\rm SSB}$ in the symmetron geodesics equation. This dependence makes the total potential that corresponds to the symmetron model to have a stronger contribution from the scalar field and thus, a larger ellipticity than the total chameleon potential. This happens even in the case that the intrinsic distribution of the symmetron field alone is more spherical.

In summary, we propose an astrophysical test which can be used as a probe to detect or differentiate screening mechanisms associated to scalar fields which are present in gravity theories that modify GR at scales larger than the Solar System. We show that the existence of such a screening mechanism can strongly affect the shape of galaxy clusters. Starting from a dark matter density distribution that corresponds to a nonspherical cluster of galaxies, we measure the shape of the isosurfaces that correspond to Newtonian potential and two scalar field models (symmetron and chameleon). We find that both scalar field models give isosurfaces that follow much more closely the density distribution than the Newtonian potential. Furthermore, we find that the shape of the isosurfaces also depends on the mechanism used to screen the fifth force: the symmetron model tends to give more spherical distributions than the chameleon one. Since present observations show some tension between the shape of real clusters [11,13]and predictions obtained from simulations [5], our results indicate that if scalar fields make any difference, it is in the right direction to correct the discrepancy in the observations.

Finally, using recent data from x-ray observations, we calculate novel constraints on the coupling β, and the ranges, $\lambda_{s,0}$ and λ_c, of the scalar fields' fifth force.

D. F. M. and C. L. L. thank the Research Council of Norway for funding, and H. Winther and H. Dahle for discussions.

[1] T. Clifton, P. G. Ferreira, A. Padilla, and C. Skordis, Phys. Rep. **513**, 1 (2012).
[2] A. Vainshtein, Phys. Lett. **39B**, 393 (1972).
[3] K. Hinterbichler and J. Khoury, Phys. Rev. Lett. **104**, 231301 (2010).
[4] J. Khoury and A. Weltman, Phys. Rev. Lett. **93**, 171104 (2004).
[5] E. T. Lau, D. Nagai, A. V. Kravtsov, and A. R. Zentner, Astrophys. J. **734**, 93 (2011).
[6] C. Llinares, Ph.D. thesis, University of Groningen, 2011, http://dissertations.ub.rug.nl/faculties/science/2011/c.llinares.
[7] J. F. Navarro, C. S. Frenk, and S. D. M. White, Astrophys. J. **490**, 493 (1997).
[8] J. C. Muñoz-Cuartas, A. V. Macciò, S. Gottlöber, and A. A. Dutton, Mon. Not. R. Astron. Soc. **411**, 584 (2011).
[9] J. Dubinski and R. G. Carlberg, Astrophys. J. **378**, 496 (1991).
[10] L. D. Shaw, J. Weller, J. P. Ostriker, and P. Bode, Astrophys. J. **646**, 815 (2006).
[11] E. T. Lau, D. Nagai, A. V. Kravtsov, A. Vikhlinin, and A. R. Zentner, Astrophys. J. **755**, 116 (2012).
[12] A. Vikhlinin *et al.*, Astrophys. J. **692**, 1033 (2009).
[13] M. Oguri, M. B. Bayliss, H. Dahle, K. Sharon, M. D. Gladders, P. Natarajan, J. F. Hennawi, and B. P. Koester, Mon. Not. R. Astron. Soc. **420**, 3213 (2012).